

# Photogelling fluids based on light-activated growth of zwitterionic wormlike micelles

Rakesh Kumar and Srinivasa R. Raghavan\*

Received 27th June 2008, Accepted 16th October 2008

First published as an Advance Article on the web 9th December 2008

DOI: 10.1039/b809452g

The creation of fluids with light-tunable rheological properties using simple, inexpensive chemicals has been a recent focus of our laboratory. Such fluids could be useful in applications ranging from sensors to microfluidic valves. Towards this end, we report in this paper a class of aqueous fluids that exhibit “photogelling”, *i.e.*, a substantial (10 000-fold) increase in fluid viscosity upon exposure to light. Such an increase in viscosity is triggered by the light-activated growth of wormlike micelles in the sample. The key components in the above fluids are the zwitterionic surfactant, erucyl dimethyl amidopropyl betaine (EDAB) and the photoresponsive molecule, *trans*-ortho-methoxy-cinnamic acid (OMCA), both of which are commercially available. OMCA binds to EDAB, and when the two are combined at high (>2 : 1) OMCA : EDAB molar ratios, short cylindrical micelles are formed in aqueous solution. Upon irradiation by UV light (<400 nm), OMCA gets photo-isomerized to its *cis* form, which then desorbs from EDAB micelles. In turn, a transition from short to long, entangled micelles ensues. Support for the above mechanism is provided by  $\zeta$  potential and small-angle neutron scattering (SANS) studies. The photogelling effect can be reversed by further addition of OMCA, allowing the sample to be cycled through high- and low-viscosity states.

## Introduction

Interest in stimuli-responsive fluids and materials has been building considerably over the past decade. A stimulus of particular focus has been light, and among the various material properties that one seeks to modulate using light are the rheological properties (such as viscosity).<sup>1,2</sup> Accordingly, several groups,<sup>1–6</sup> including ours,<sup>7</sup> have sought to create fluids whose viscosity can be modulated by irradiation with light at a given wavelength. Such fluids could properly be termed *photo-rheological* (PR) fluids,<sup>7,8</sup> a term that was originally introduced into the literature by Wolff and co-workers<sup>8</sup> in the late 1980s. Much of the interest in developing PR fluids has been due to their potential to be used in microscale applications, such as microvalves or flow sensors within or microfluidic devices.<sup>7</sup> In such applications, the use of light as a modulating field can be particularly advantageous since light can be directed at a precise spot with resolution of a few micrometers.

Our approach to PR fluids has differed from those of others in an important way. The focus of other groups has largely been on synthesizing novel light-sensitive organic molecules, such as new classes of photoresponsive surfactants<sup>1,3,4</sup> or polymers,<sup>5,6</sup> and using these to create the PR fluids. While these studies have demonstrated impressive rheology-modulation with light, the light-sensitive molecules underlying these systems have remained accessible only to the select groups that are capable of synthesizing them. We have instead sought to create PR fluids from simple, existing molecules that would be available to any

chemistry laboratory. In a recent study,<sup>7</sup> we have shown that such an idea is feasible: specifically, we reported PR fluids that were mixtures of two widely available chemicals: the cationic surfactant, cetyl trimethylammonium bromide (CTAB) and the photoisomerizable molecule, *trans*-ortho-methoxy-cinnamic acid (OMCA). We showed that CTAB–OMCA fluids undergo *photothinning*, *i.e.*, a rapid and controllable decrease in viscosity (factors of 1000 to 10 000) upon exposure to UV radiation.<sup>7</sup> This viscosity change was not reversible by light, *i.e.*, the viscosity could be decreased but not increased. Despite this limitation, our study did show that dramatic light-triggered rheological changes are possible in simple systems. From a mechanistic standpoint, the molecular change (*trans*–*cis* isomerization of OMCA) underlying the phenomenon was connected to changes in the microstructure (reductions in the size of wormlike micelles), and thereby to the drop in viscosity.<sup>7</sup>

In this paper, we describe a new class of PR fluids that exhibit *photogelling*, *i.e.*, a 10 000-fold increase in viscosity upon UV irradiation. These fluids again consist of two commercial compounds: the zwitterionic surfactant, erucyl dimethyl amidopropyl betaine (EDAB) and the same photoadditive as before, *i.e.*, OMCA. The main results, as indicated by Fig. 1, are that certain mixtures of EDAB and OMCA form fluids with a low viscosity (similar to water). Upon UV irradiation, OMCA is converted from its *trans* to its *cis* form,<sup>7</sup> and in turn, these fluids are transformed into highly viscous, gel-like samples. We will show that the rheological changes correlate with a transition from short to long, “wormlike” micelles.<sup>9,10</sup> In other words, the light-induced change in OMCA geometry *activates the axial growth* of cylindrical micelles into long, flexible chains that undergo physical entanglement, producing a viscoelastic fluid. Although the photogelling cannot be reversed by light (see

Department of Chemical & Biomolecular Engineering, University of Maryland, College Park, MD 20742-2111. E-mail: sraghava@eng.umd.edu

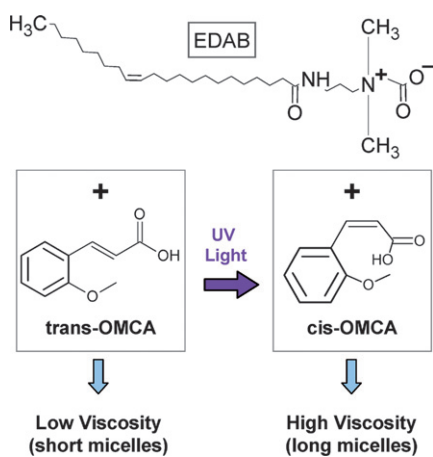


**Fig. 1** The composition of photogelling fluids described in this paper. The fluids consist of the zwitterionic surfactant, EDAB and the organic derivative, OMCA. When EDAB is combined with *trans*-OMCA, the result is a low-viscosity fluid. Upon UV irradiation, *trans*-OMCA is photoisomerized to *cis*-OMCA, which causes a substantial rise in fluid viscosity. The viscosity rise is associated with the growth of EDAB micelles.

discussion later), we will show that the viscosity *can* be decreased by further addition of OMCA. Thus, a combination of light and sample composition can be used to cycle the viscosity between high and low states.

A few further points are worth mentioning at this stage. First, the change from a photothinning system (our earlier study) to the photogelling system described here is not a trivial one. Specifically, photogelling requires the use of a zwitterionic surfactant that is capable of forming wormlike micelles (“worms” for short).<sup>11,12</sup> Although zwitterionic surfactants, including EDAB, are popular in industry due to their low skin irritation and biodegradability,<sup>13</sup> they have not been investigated in detail by academic researchers. Most academic studies on wormlike micelles have utilized cationic surfactants like CTAB, and for those surfactants to form worms it is well known that salts—either inorganic or organic—must be added.<sup>9,10</sup> On the other hand, EDAB is a long (C<sub>22</sub>-tailed) zwitterionic surfactant that can form worms even in the absence of salt—in fact, inorganic salts like NaCl have no influence on worm formation.<sup>12</sup> These aspects of the rheology of EDAB worms were brought to light in our recent paper<sup>12</sup> that may be considered a precursor to the present study.

It is worth reiterating that EDAB and similar betaine surfactants are commercially available,<sup>12</sup> allowing researchers in any lab to replicate our results and to use photogelling fluids for applications of interest. Interestingly, from an applications standpoint, photogelling is likely to be more useful than photothinning—one potential application would be in capillary electrophoresis, where a photogelling carrier fluid can be loaded into the capillary while it is thin and later transformed into a gel-like state by UV irradiation. Also, in the context of biomolecular applications such as bioseparations, EDAB-based PR fluids may indeed be formulated using physiological buffer solutions. Note that the background electrolyte in such buffers does not influence micelle formation in the case of EDAB or

other zwitterionics,<sup>11,12</sup> but would do so in the case of cationic surfactants.<sup>9,10</sup>

Finally, we wish to elaborate a bit more on the mechanism underlying the photogelling reported in this paper (a detailed discussion is given later). The key to the mechanism is that (a) EDAB is zwitterionic; and (b) the *trans* isomer of OMCA tends to bind and intercalate into EDAB micelles, whereas the *cis* isomer does not. When binding occurs, an effective charge is imparted to EDAB headgroups, which translates into short micelles. On the other hand, when the *cis* isomer unbinds and exits the micelle, the effective charge is reduced, causing micellar growth (see Fig. 7 later). Indeed, we have been able to verify this mechanism through a combination of small-angle neutron scattering (SANS) and  $\zeta$  potential measurements. SANS is a sensitive probe for the dimensions of the micelles, while  $\zeta$  potential probes the net surface charge on the micelles. In sum, the photoinduced rheological transitions reported in this paper can be sensibly explained by the coupling of events occurring at the molecular, microstructural, and macroscopic scales.

## Experimental section

### Materials

The EDAB surfactant was a commercial product manufactured by Rhodia Inc., Cranbury, NJ. EDAB is a zwitterionic surfactant of the betaine type (see structure in Fig. 1), with the molecule having both a positively charged dimethylammonium moiety and a negatively charged carboxylate group. Further details about the sample are given in our earlier paper; as an aside, the critical micelle concentration (CMC) of EDAB is very low:  $\sim 1 \mu\text{M}$ .<sup>12</sup> OMCA in its *trans* form was purchased from Acros Chemicals, while the *cis* form was purchased from TCI America (each isomer was greater than 98% in purity). Ultra-pure deionized water from a Millipore water-purification system was used in preparing samples for rheological characterization, while D<sub>2</sub>O (99.95% deuteration, from Cambridge Isotopes) was used for the SANS studies. Solutions containing OMCA were buffered to a pH of 10 using equimolar amounts of sodium carbonate and sodium bicarbonate. Weighed quantities of EDAB were added to these solutions to reach the final sample compositions. Samples were stirred continuously under mild heat until they became homogeneous. The solutions were then left to equilibrate overnight at room temperature before conducting any experiments.

### Sample response before and after UV irradiation

EDAB–OMCA samples were irradiated with UV light from a Oriel 200 W mercury arc lamp. A dichroic beam turner with a mirror reflectance range of 280 to 400 nm was used to access the UV range of the emitted light. Samples (5 mL) were placed in a Petri dish with a quartz cover and were irradiated for a specific duration under stirring. Due to the nature of the OMCA spectra, irradiated samples did not undergo any changes when stored under ambient conditions, which made it easy to conduct subsequent tests.

## Rheological studies

Steady and dynamic rheological experiments were performed on an AR2000 stress controlled rheometer (TA Instruments, Newark, DE). Samples were run at 25 °C on a cone-and-plate geometry (40 mm diameter, 2° cone angle) or a Couette geometry (rotor of radius 14 mm and height 42 mm, and cup of radius 15 mm). Dynamic frequency spectra were obtained in the linear viscoelastic regime of each sample, as determined by dynamic stress-sweep experiments.

## Small angle neutron scattering (SANS)

SANS measurements were taken on the NG-7 and NG-3 (30 m) beamlines at NIST in Gaithersburg, MD. Neutrons with a wavelength of 6 Å were selected. Three sample-detector distances were used to obtain data over a range of wave vectors from 0.004 to 0.4 Å<sup>-1</sup>. Samples were studied in 2 mm quartz cells at 25 °C. Scattering spectra were corrected and placed on an absolute scale using NIST calibration standards. The data are shown as plots of the absolute intensity  $I$  versus the wave vector  $q = 4\pi\sin(\theta/2)/\lambda$ , where  $\lambda$  is the wavelength of incident neutrons and  $\theta$  the scattering angle.

## SANS data analysis

SANS data were analyzed by the Indirect Fourier Transform (IFT) method, which requires no *a priori* assumptions on the nature of the scatterers.<sup>14</sup> Here, a Fourier transformation of the scattering intensity  $I(q)$  is performed to obtain the pair distance distribution function  $p(r)$  in real space.  $p(r)$  provides structural information about the scatterers, such as their maximum dimension. IFT analysis was implemented using the commercial PCG software package.

## $\zeta$ potential

The  $\zeta$  potential of EDAB-OMCA micelles was measured for dilute solutions using a Zetasizer 3000HS (Malvern Instruments). The electrophoretic mobility was measured and converted into the  $\zeta$  potential using the Smoluchowski equation.<sup>15</sup> Prior to use with our samples, the instrument was calibrated using  $\zeta$  potential transfer standards. Each reported value is an average over 9 independent measurements.

## Results and discussion

We first discuss the differences between *trans* and *cis*-OMCA when combined with solutions of EDAB. As mentioned earlier, OMCA is available commercially in both its *trans* and *cis* forms, permitting separate studies with each isomer. When EDAB alone is added to water at a concentration of 50 mM, it turns it into a gel-like fluid. The rheology of EDAB samples at various concentrations has been reported in detail in our previous paper.<sup>12</sup> Fig. 2 shows that a 50 mM EDAB solution (no OMCA) has a low-shear viscosity of about 300 Pa s. When *cis*-OMCA is added to the EDAB solution, it has negligible effect on the rheology and the viscosity stays practically unchanged over the entire range of *cis*-OMCA concentrations (○). In contrast, the addition of *trans*-OMCA lowers the viscosity

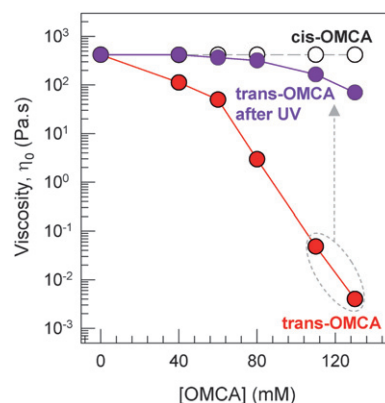


**Fig. 2** Zero-shear viscosity  $\eta_0$  of 50 mM EDAB-OMCA mixtures as a function of the OMCA concentration. Data are shown for samples containing either *trans*-OMCA or *cis*-OMCA and for *trans*-OMCA samples after 20 min of UV irradiation. As shown by the arrow, the high *trans*-OMCA samples undergo photogelling, *i.e.*, they experience a significant light-induced increase in viscosity.

of EDAB solutions: about 130 mM of *trans*-OMCA reduces the viscosity to a value close to that of water (1 mPa s). This result is similar to that reported in our earlier paper,<sup>12</sup> where we had studied the effects of adding salts to EDAB solutions. While simple, inorganic salts like NaCl were not found to have an effect on EDAB solution rheology, aromatic salts like sodium salicylate (NaSal) and sodium hydroxy-naphthalene-carboxylate (NaHNC) both reduced the viscosity. The viscosity reduction was much higher for the more hydrophobic counterion, *i.e.*, NaHNC compared to NaSal.<sup>12</sup> The mechanism underlying such viscosity reduction is discussed later in the paper.

For the moment, we will highlight the effect of UV irradiation on EDAB + *trans*-OMCA samples. As discussed in our earlier study on PR fluids,<sup>7</sup> *trans*-OMCA gets photoisomerized to *cis*-OMCA upon UV irradiation (UV-Vis spectra are reported in the above paper and are not repeated here). It is therefore of interest to examine the changes in the rheology of EDAB-*trans*-OMCA solutions upon UV irradiation. Accordingly, we irradiated each of the above samples for 20 min and then recorded their rheological responses. Note that, following irradiation, the samples remained unaltered when stored under ambient conditions (exposure to visible light has no effect because both OMCA isomers have no measurable absorbance in the visible range of the spectrum<sup>7</sup>). Thus, irradiated samples could be conveniently tested by rheometry, and their zero-shear viscosity  $\eta_0$  values are shown in Fig. 2. All samples exhibit an increase in  $\eta_0$ , with the increase being particularly significant (factor of 10 000 or more) for samples having a high *trans*-OMCA content. The latter samples will be the focus of the rest of the paper, and we will describe their light-induced transformation as “photogelling”.

Fig. 3 shows photographs and dynamic rheological data for a photogelling sample consisting of 50 mM EDAB and 130 mM *trans*-OMCA. Before UV irradiation, the sample is a freely flowing, low-viscosity liquid that readily pours out of the vial. Upon UV irradiation, it is clear that the sample has been converted into a viscoelastic, gel-like fluid (note the presence of entrapped bubbles). Flow-birefringence, *i.e.*, bright streaks of light under crossed polarizers, was also seen when this gel-like

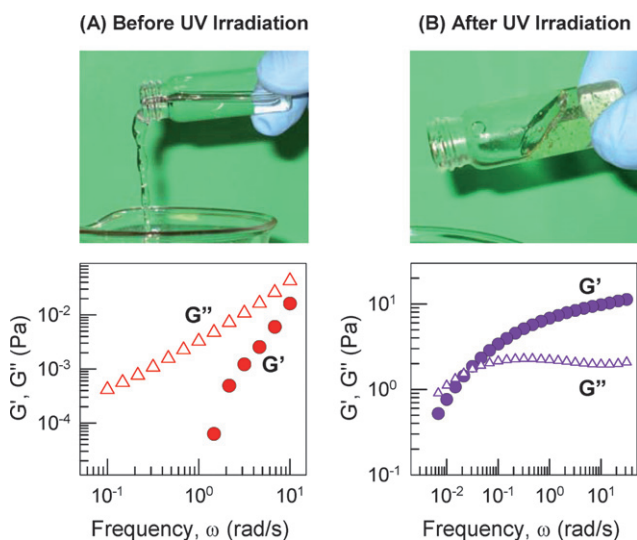


**Fig. 3** Photographs and dynamic rheological data (frequency spectra) for a sample containing 50 mM EDAB + 130 mM *trans*-OMCA (A) before and (B) after UV irradiation. Before irradiation, the sample is water-like and shows a purely viscous response in dynamic rheology. After UV irradiation for 30 min, the sample is gel-like and shows a strongly viscoelastic response. Note that the latter sample does not flow easily out of the tilted vial and also note the presence of trapped bubbles in the fluid.

sample was shaken. No such flow-birefringence was evident before UV irradiation. As is well-known, strong viscoelasticity and flow-birefringence are characteristic properties of surfactant samples that contain wormlike micelles, *i.e.*, long and flexible micellar chains with a cylindrical cross-section.<sup>9,10</sup> Thus visual evidence points to the existence of wormlike micelles in the sample after UV irradiation.

The above visual observations are fully consistent with the dynamic rheological data shown in Fig. 3. The data are presented as plots of the elastic modulus  $G'$  and viscous modulus  $G''$  vs. the angular frequency  $\omega$ . The sample before irradiation behaves like a viscous liquid over the entire range of frequencies (*i.e.*, in this case,  $G'' > G'$ , with both moduli being strong functions of frequency). On the other hand, the irradiated sample shows a strongly viscoelastic response, *i.e.* the response is elastic over most of the frequency range ( $G' > G''$ , plateau in  $G'$ ), whereas it is viscous at very low frequencies or long time scales. The frequency at which  $G'$  and  $G''$  intersect is an estimate for the longest relaxation time of the sample, which is about 100 s in this case. This relaxation time is more than a factor of 1000 higher than that of the unirradiated sample. Note that the irradiated material is gel-like, but not a “true” gel—if so, the relaxation time would be infinite and the moduli would never intersect.

The light-induced rheological changes are also evident under steady-shear rheology. Fig. 4 shows viscosity vs. shear rate plots for the 50 mM EDAB + 130 mM *trans*-OMCA sample after various intervals of UV irradiation. Before UV irradiation, the sample is a low-viscosity, Newtonian fluid. After 10 min of irradiation, the zero-shear viscosity  $\eta_0$  is increased by two orders of magnitude and the sample shows shear-thinning at high shear rates. After 20 min,  $\eta_0$  is further increased by another two orders of magnitude and the sample becomes strongly shear-thinning.

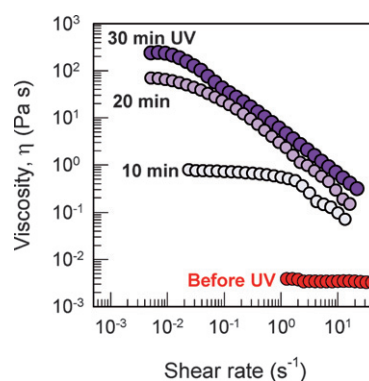


**Fig. 4** Steady-shear rheology of a 50 mM EDAB + 130 mM *trans*-OMCA sample before irradiation and after UV irradiation for various periods of time (as indicated on the plot). The sample is observed to switch from a low-viscosity, Newtonian fluid to a highly viscous, shear-thinning fluid with progressive irradiation.

After 30 min,  $\eta_0$  is close to that of a 50 mM EDAB sample with *cis*-OMCA and no further increase in  $\eta_0$  occurs with longer irradiation. The viscosity increase is thus tunable *via* the irradiation time. It should be noted that the *rate-limiting step for photogelling is the rate of absorption of UV light by the sample* (the photoisomerization itself occurs in milliseconds).<sup>7</sup> In turn, light absorption depends on the intensity of the UV lamp, the sample volume, and the experimental geometry (path length). Rapid transitions can be easily achieved for small sample volumes confined in thin channels.

The results thus far have shown a significant light-induced viscosity increase (photogelling) in EDAB + *trans*-OMCA samples and have been attributed to a transition from short to long wormlike micelles. To confirm this hypothesis, we resorted to SANS. Samples were made in  $D_2O$  for SANS experiments to attain the required contrast between micellar structures and solvent (the switch from  $H_2O$  to  $D_2O$  had no effect on the sample rheology). Fig. 5 shows SANS spectra for 50 mM EDAB solutions at three different *trans*-OMCA concentrations: 150, 170, and 190 mM, respectively. Data are shown both before and after UV irradiation for 30 min. All samples show a significant rise in low- $q$  scattering intensity upon irradiation. This rise in low- $q$  intensity indicates an increase in micellar size. For the 170 and 190 mM *trans*-OMCA samples (Fig. 5b and 5c), before irradiation, there is a plateau in the low- $q$  intensity, suggesting the presence of spherical micelles (or ellipsoids with nearly equal long and short axes). On the other hand, after irradiation, there is a  $q^{-1}$  decay of the intensity at low  $q$ , which is indicative of scattering from long cylindrical chains. There is also no appreciable change in the intensity at high  $q$  upon UV irradiation, which implies that the micellar radius remains the same before and after irradiation.

Further quantitative information from the SANS data can be obtained by modeling it through the Indirect Fourier Transform (IFT) method.<sup>14</sup> Using IFT, we can analyze our SANS data without assuming *a priori* the nature of the scatterers, *e.g.*, whether micelles are long or short, cylindrical or spherical. IFT modeling of the SANS data from the 50 mM EDAB + 190 mM *trans*-OMCA sample yielded the pair distance distribution functions  $p(r)$  shown in Fig. 5d. Before irradiation,  $p(r)$  is

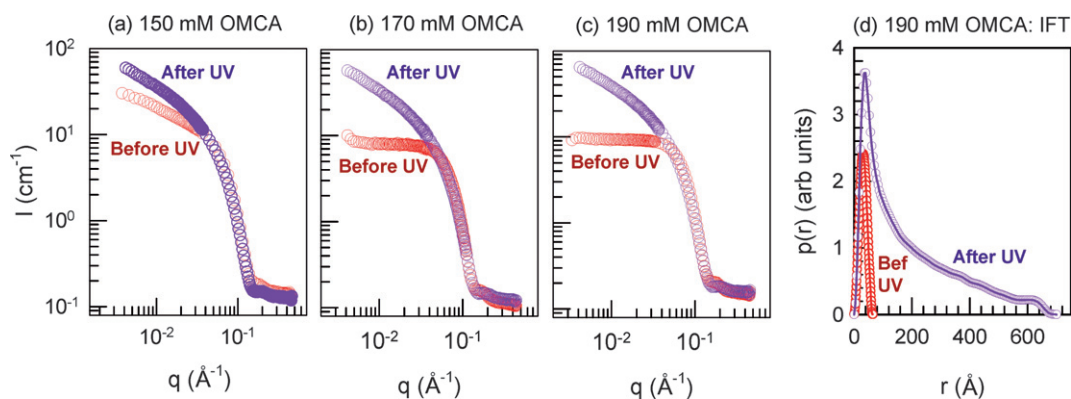


**Fig. 5** SANS data and analysis for EDAB–*trans*-OMCA mixtures before and after 30 min of UV irradiation. Plots (a)–(c) show scattering spectra (intensity  $I$  vs. wave vector  $q$ ) for three samples, each with 50 mM EDAB and with OMCA concentrations of 150, 170, and 190 mM, respectively. Plot (d) presents an analysis of the data for the 190 mM OMCA sample using the IFT method. See text for details.

symmetrical with a narrow peak. This symmetry suggests small spherical micelles with a diameter of about 65 Å (the diameter corresponds to the point where  $p(r)$  meets the  $x$ -axis). In contrast, after irradiation  $p(r)$  is asymmetrical and decreases to zero around 700 Å. This  $p(r)$  function is characteristic of long cylindrical micelles. The point where  $p(r)$  meets the  $x$ -axis is a lower estimate for the contour length of the cylinders, *i.e.*, 700 Å in this case. Thus, the SANS data confirm that the microstructural basis for photogelling involves the light-induced growth of cylindrical micelles.

The key question now is to connect the light-induced microstructural transition (short to long micelles) with the transitions occurring at the molecular level. As discussed in our earlier study, we have confirmed that the main effect of light at the molecular level is to induce a *trans* to *cis* photoisomerization of OMCA.<sup>7,16</sup> Other photoinduced effects associated with cinnamic acid or its derivatives such as photodimerization<sup>16</sup> have been ruled out using high-performance liquid chromatography (HPLC).<sup>7</sup> We had also shown that *trans*-OMCA is significantly more hydrophobic than *cis*-OMCA. One piece of evidence in this regard was the solubility of the two isomers in deionized water: while the solubility of *cis*-OMCA was 8.6 mM, that of *trans*-OMCA was only 0.26 mM *i.e.*, more than a factor of 30 less.<sup>7</sup> This finding is consistent with other studies that have found the *trans* isomer to be more hydrophobic than the *cis* isomer for a variety of other compounds.<sup>3,4</sup> In the present context, the hydrophobicity of *trans*-OMCA implies that it will readily bind (intercalate) to EDAB micelles, whereas the more hydrophilic *cis*-OMCA will be more likely to remain in solution.

The tendency of *trans*-OMCA to bind to EDAB micelles while *cis*-OMCA does not is central to our proposed mechanism. We further postulate that counterion binding regulates micellar growth through its effect on micellar surface (headgroup) charge. As stated in the Introduction, EDAB is a zwitterionic surfactant, and the low charge on the EDAB headgroup (coupled with the long C<sub>22</sub> tail length) facilitates the formation of worms.<sup>12</sup> If an anionic counterion like *trans*-OMCA were to bind to EDAB worms, the result would be to impart a net negative charge to the headgroup. The resulting charge repulsions would expand the EDAB headgroup area.<sup>15</sup> In turn, the molecular geometry would now favor the formation of short cylinders or spheres rather than

long cylinders (worms). The micelles would thereby tend to become much shorter, explaining the low viscosity of EDAB + *trans*-OMCA samples.

In order to test our above hypothesis, we turn to  $\zeta$  potential measurements (Fig. 6). The  $\zeta$  potential quantifies the surface charge densities of colloidal particles. We studied the surface charge on EDAB micelles before and after adding OMCA. The concentrations were kept low (2.5 mM EDAB and 0 to 5 mM of *trans*- and *cis*-OMCA) in order to minimize the effects of micelle size, shape, and intermicellar interactions.<sup>15</sup> Significantly, the  $\zeta$  potential results show the very same trends seen previously in the viscosity data (compare Fig. 2 and 6). In Fig. 6, we note that the zwitterionic EDAB micelles have a low surface charge and hence a low  $\zeta$  potential of  $-22.9$  mV. When *cis*-OMCA is added to the solution, the  $\zeta$  potential is practically unchanged, indicating that the *cis* isomer is not bound to the micelles. However, with increasing amounts of *trans*-OMCA, the  $\zeta$  potential becomes more and more negative: the values go from  $-22.9$  to  $-53.6$  mV as *trans*-OMCA is increased from 0 to 5 mM. The implication is that *trans*-OMCA binds (intercalates) to EDAB micelles, thereby making their surface more negative. Finally, we show results for

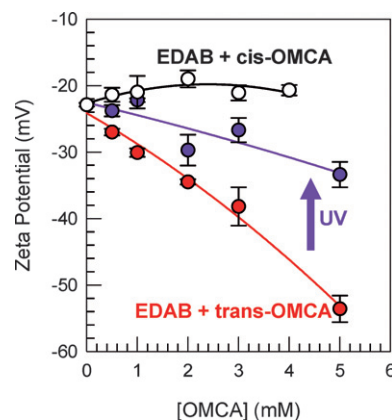


**Fig. 6** The  $\zeta$  potential of 2.5 mM EDAB–OMCA mixtures as a function of the OMCA concentration. Data are shown for *trans*-OMCA, *cis*-OMCA, and *trans*-OMCA samples after 30 min of UV irradiation. Lines through the data are guides for the eye.

EDAB–*trans*-OMCA samples after 20 min of UV irradiation. In all cases, the irradiated samples show less negative  $\zeta$  potentials, indicating that the surface charge on the micelles has been lowered. This is fully consistent with the idea that photoisomerization of *trans*-OMCA to *cis*-OMCA leads to unbinding of the latter from EDAB micelles.

The  $\zeta$  potential data validate our hypothesis that counterion binding and the resulting electrostatic effects are the underlying basis for photogelling in the present system. The key point is that *trans*-OMCA has a much greater affinity for EDAB micelles than *cis*-OMCA. The reason for this has to do with the greater hydrophobicity of *trans*-OMCA (see above) and also its favorable geometry.<sup>7</sup> With regard to geometry, the hydrophobic and hydrophilic parts of *trans*-OMCA are well separated, allowing the counterion to intercalate its hydrophobic parts (aromatic ring, methyl group) into the micelle interior while exposing its hydrophilic part (carboxylate anion) to the water outside. On the other hand, the methyl and carboxylate groups are located very close to each other in the case of *cis*-OMCA, which makes it difficult for the counterion to bind in a way that would be favorable to the entire molecule. Therefore, from a geometry standpoint also, one expects *trans*-OMCA to have a much stronger tendency to bind (intercalate) into zwitterionic micelles than *cis*-OMCA.

Taken together, photogelling can be explained based on the schematics shown in Fig. 7. At the molecular level, *trans*-OMCA binds to EDAB micelles, increasing the charge on the headgroup and thereby the effective headgroup size. The effective geometry

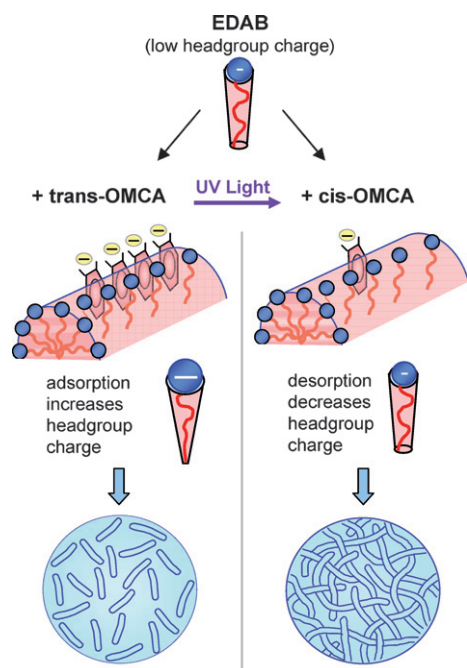


**Fig. 7** Mechanism for photogelling in EDAB samples. Addition of *trans*-OMCA increases the effective headgroup charge due to adsorption of the counterions, and this leads to short micelles. When *trans*-OMCA is photoisomerized to *cis*-OMCA, the *cis* isomer desorbs from the micelles, effectively lowering the headgroup charge. As a result, the micelles grow into long, wormlike structures, and the viscosity thereby increases substantially (photogelling).

thus goes from a truncated cone in the case of EDAB to a cone shape in the case of EDAB–*trans*-OMCA. As a result, small micelles (spheres or short cylinders) are formed. When *trans*-OMCA is photoisomerized to *cis*-OMCA, the latter unbinds and exits the micelles. The headgroup charge is decreased to its original low value, and the molecular geometry reverts to a truncated cone shape. Accordingly, the micelles grow into long cylinders and the increase in their contour length  $L$  sharply increases the timescale for worm reptation or dis-entanglement ( $t_{\text{rep}} \sim L^3$ ).<sup>9</sup> This explains why longer worms lead to a viscosity increase (photogelling).

Finally, we wish to explore the reversibility of the viscosity changes in EDAB–OMCA systems. As discussed in our earlier paper,<sup>7</sup> a reverse *cis* to *trans* photoisomerization is not possible with OMCA because the absorbance of the *cis* isomer is lower than that of the *trans* over most of the UV and visible wavelength ranges. Nevertheless, photogelling in EDAB–OMCA fluids can indeed be reversed by a composition change. Specifically, after the sample has been photogelled, we can reduce its viscosity by adding more *trans*-OMCA to it. This is shown in Fig. 8, where the viscosity is taken along multiple cycling steps: in each step, the upward cycle is caused by UV irradiation at constant composition while the downward cycle is caused by a composition change. Such viscosity cycling can be done up to 2 times.

The above ability to cycle the viscosity demonstrates several things: first, it shows that the viscosity change is indeed connected to self-assembly phenomena, not covalent bond formation or other irreversible processes. Second, the reason this works is very much consistent with our postulated mechanism. Take cycle 1 as an example: during the upward cycle, *trans*-OMCA bound to the micelles is converted to *cis*-OMCA, which desorbs from the micelles. Then, more *trans*-OMCA is added to the solution, which binds to the micelles and increases their charge, lowering the viscosity. In the next cycle, the process is repeated, *etc.* Note that cycling cannot be done indefinitely because the photo-conversion of *trans* to *cis* only proceeds up to a photostationary state of 80% *cis*.<sup>7</sup> Also, samples with more

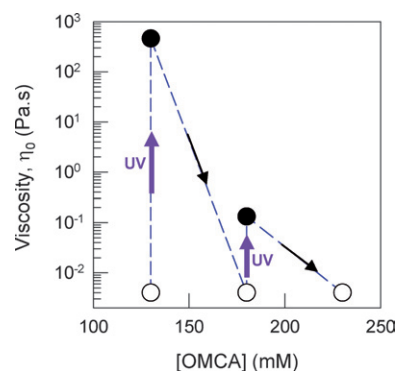


**Fig. 8** The cycling of viscosity by UV irradiation and sample composition. The initial sample (50 mM EDAB + 130 mM *trans*-OMCA) is exposed to UV light for 40 min, causing a 10 000-fold rise in viscosity. Then, 50 mM *trans*-OMCA is added, which drops the viscosity back to its original value. The resulting sample is then irradiated again for 40 min, which induces a 50-fold increase in viscosity. Finally, the addition of a further 50 mM of *trans*-OMCA again decreases the viscosity back to its original value.

*trans*-OMCA require longer times to increase their viscosity, which is why the “high” viscosity is lower in the second cycle than the first (the same irradiation time was used for all samples). At any rate, using the above methodology, it is indeed possible to go back and forth between high and low viscosity states, and this is an aspect that could be useful in certain applications.

From an applications standpoint, we should reiterate that the present photoresponsive fluid based on a zwitterionic surfactant offers some advantages over those based on ionic surfactants. In particular, photogelling EDAB–OMCA fluids are quite tolerant to the addition of other components, such as electrolytes, macromolecules, or nanoparticles. An application that could be of interest for photogelling fluids is in capillary electrophoresis, as mentioned in the Introduction. Other applications are bound to arise once photogelling fluids are more widely studied; again, the facile preparation of these fluids from inexpensive commercial ingredients should allow new investigators to venture into this field.

## Conclusions

We have shown that UV irradiation can induce a dramatic increase in viscosity (*i.e.*, photogelling) in EDAB–OMCA mixtures. The step-by-step mechanism for this phenomenon is as follows: (1) EDAB, a zwitterionic surfactant (low head group charge, long tail) forms long wormlike micelles in water, which gives rise to a very high viscosity. (2) When OMCA is in its *trans* form, it binds strongly to EDAB due to its high hydrophobicity and favorable geometry. The binding of these anionic counterions, in turn, increases the headgroup charge and thereby headgroup repulsions. This causes a dramatic reduction in micelle size, and thus in solution viscosity. (3) Upon irradiation by UV light, *trans*-OMCA is isomerized to *cis*-OMCA. The *cis* isomer has a much weaker interaction with EDAB since its geometry and lesser hydrophobicity do not favor binding at the micellar interface. Thus, the *cis* isomer tends to desorb from the micellar

interface, allowing the spherical micelles to transform back into long wormlike micelles. The solution viscosity thus increases by more than four orders of magnitude.

## Acknowledgements

This work was funded by a CAREER award from NSF-CTS. We acknowledge NIST NCNR for enabling the SANS experiments performed as part of this work. We are also thankful to Dr Hamid Ghandehari of the UM Pharmacy School at Baltimore for facilitating the  $\zeta$  potential studies.

## References

- 1 J. Eastoe and A. Vesperinas, *Soft Matter*, 2005, **1**, 338–347.
- 2 J. M. J. Paulusse and R. P. Sijbesma, *Angew. Chem., Int. Ed.*, 2006, **45**, 2334–2337.
- 3 C. T. Lee, K. A. Smith and T. A. Hatton, *Macromolecules*, 2004, **37**, 5397–5405.
- 4 H. Sakai, Y. Orihara, H. Kodashima, A. Matsumura, T. Ohkubo, K. Tsuchiya and M. Abe, *J. Am. Chem. Soc.*, 2005, **127**, 13454–13455.
- 5 I. Tomatsu, A. Hashidzume and A. Harada, *Macromolecules*, 2005, **38**, 5223–5227.
- 6 G. Pouliquen and C. Tribet, *Macromolecules*, 2006, **39**, 373–383.
- 7 A. M. Ketner, R. Kumar, T. S. Davies, P. W. Elder and S. R. Raghavan, *J. Am. Chem. Soc.*, 2007, **129**, 1553–1559.
- 8 T. Wolff, C. S. Emming, T. A. Suck and G. Von Bunau, *J. Phys. Chem.*, 1989, **93**, 4894–4898.
- 9 M. E. Cates and S. J. Candau, *J. Phys.: Condens. Matter*, 1990, **2**, 6869–6892.
- 10 C. A. Dreiss, *Soft Matter*, 2007, **3**, 956–970.
- 11 T. Shikata and S. Itatani, *Colloid Polym. Sci.*, 2003, **281**, 447–454.
- 12 R. Kumar, G. C. Kalur, L. Ziserman, D. Danino and S. R. Raghavan, *Langmuir*, 2007, **23**, 12849–12856.
- 13 J. Yang, *Curr. Opin. Colloid Interface Sci.*, 2002, **7**, 276–281.
- 14 O. Glatter, *J. Appl. Crystallogr.*, 1977, **10**, 415–421.
- 15 P. C. Hiemenz and R. Rajagopalan, *Principles of Colloid and Surface Chemistry*, Marcel Dekker, New York, 3rd edn, 1997.
- 16 T. Imae, T. Tsubota, H. Okamura, O. Mori, K. Takagi, M. Itoh and Y. Sawaki, *J. Phys. Chem.*, 1995, **99**, 6046–6053.